EUROPEAN ORGANIZATION FOR NUCLEAR RESEARCH

ALEPH 94-133
PHYSIC 94-116
July 26, 1994
P. Campana *et al.*

Determination of the upper limit on the τ neutrino mass from $\tau \rightarrow 5\pi^{\pm}(\pi^{o})\nu_{\tau}$ decays

P. Campana[1], F. Cerutti[1], L. Passalacqua[2]

Abstract

Following a method developed inside ALEPH an upper limit of 23.8 MeV/c^2 at 95% CL on the τ neutrino mass has been measured. A maximum likelihood fit in the hadronic (mass,energy) variables has been applied to 23 $\tau \rightarrow 5\pi^{\pm}\nu_{\tau}$ and 2 $\tau \rightarrow 5\pi^{\pm}\pi^{o}\nu_{\tau}$ events selected over the 1991,1992 and 1993 data. If the standard mass end-point technique were used the limit would be 40.6 MeV/c^2 at 95% CL.

[1]Laboratori Nazionali dell'INFN, LNF-INFN , I-00044 Frascati, Italy
[2]LPNHE, Ecole Polytechnique, $IN^2P^3 - CNRS$, F-91128 Palaiseau Cedex, France

1 Introduction

Limits on the tau neutrino mass have already been given by several collaborations. All present results use the invariant mass end-point technique applied to different tau decay modes. The best results are obtained by ARGUS [1] that gives a limit of 31 MeV at 95% CL with 20 $\tau \rightarrow 5\pi^{\pm}\nu_{\tau}$ events, and CLEO II [2] that gives 32.6 MeV at 95% CL with 60 $\tau \rightarrow 5\pi^{\pm}\nu_{\tau}$ and 53 $\tau \rightarrow 3\pi^{\pm}2\pi^{o}\nu_{\tau}$ events. The CLEO II result for the five prongs mode alone is 47.5 MeV.

In this note we will make use of the standard technique and of a second method developed in ALEPH at an earlier stage [3] when a result of 60 MeV was given with a sample of 7 events (6 $\tau \rightarrow 5\pi^{\pm}\nu_{\tau}$ and 1 $\tau \rightarrow 5\pi^{\pm}\pi^{o}\nu_{\tau}$) selected over the 1989 and 1990 data. This method has the advantage of using the energy distribution of the hadronic system in addition to the invariant mass distribution, the two variables being correlated with an average factor of +0.54.

2 The method

The limit on the mass is derived from a maximum likelihood function giving the probability density of obtaining the observed distribution, either in the invariant mass alone as in the standard technique, or in the plane ($x = \frac{m_{had}}{m_{\tau}}, y = \frac{E_{had}}{E_{beam}}$). In the second case, for each a given event i, the function takes the form :

$$P_i(m_\nu) = \frac{\int_{x_m}^{x_M(m_\nu)} \int_{E_{\tau m}}^{E_{\tau M}} \mathcal{G}(E_\tau) \int_{y_m(E_\tau,m_\nu)}^{y_M(E_\tau,m_\nu)} \frac{d^2\Gamma(x,y,m_\nu)}{dxdy} \mathcal{R}(x-x_i, y-y_i)\epsilon(x,y)dxdE_\tau dy}{\int_{x_m}^{x_M(m_\nu)} \int_{y_m(E_{beam},m_\nu)}^{y_M(E_{beam},m_\nu)} \frac{d^2\Gamma(x,y,m_\nu)}{dxdy} \epsilon(x,y)dxdy}$$

Where :

- $\frac{d^2\Gamma(x,y,m_\nu)}{dxdy}$ is the theoretical distribution of the given decay mode ($5\pi^{\pm}$ or $5\pi^{\pm}\pi^{o}$);
- $\mathcal{R}(x-x_i, y-y_i)$ is the resolution function accounting for detector effects, which is taken to be a double gaussian plus a very small flat tail :

$$\mathcal{R}(x-x_i, y-y_i) = \frac{\frac{e^{-\frac{1}{2}\frac{1}{1-\rho_i^2}[(\frac{x-x_i}{\sigma_{x_i}})^2 + (\frac{y-y_i}{\sigma_{y_i}})^2 - 2\rho_i(\frac{x-x_i}{\sigma_{x_i}})(\frac{y-y_i}{\sigma_{y_i}})]}}{2\pi\sigma_{x_i}\sigma_{y_i}\sqrt{1-\rho_i^2}} + k(i)}{N(i)}$$

  with $N(i)$ such that : $\int dx \int dy \mathcal{R}(x-x_i, y-y_i) = 1$

- $\mathcal{G}(E_{beam}, E_\tau)$ is the initial state radiation function derived from one of the standard Lep formulations [4], with the assumption that the radiation is emitted along the beam pipe direction and a random choice of the emission side (i.e. e^+ or e^-);

- $\epsilon(x,y)$ is the selection efficiency, which turns out to be a constant;
- $(x_m, x_M) = (\frac{\sum_i^{5(6)} m_\pi}{m_\tau}, \frac{m_\tau - m_\nu}{m_\tau})$ are the integration limits in x and similarly :
- $(y_m, y_M) = (\frac{E^*(1-\beta\sqrt{1-(\frac{m_{had}}{E^*})^2})}{m_\tau}, \frac{E^*(1+\beta\sqrt{1-(\frac{m_{had}}{E^*})^2})}{m_\tau})$, $E^* = \frac{m_\tau^2 + m_{had}^2 - m_\nu^2}{2m_\tau}$;
- $(E_{\tau m}, E_{\tau M}) = (m_{tau}, E_{beam})$.

The above integration limits are fixed by the kinematics assuming a two body decay of the τ in the hadronic system and the neutrino. In absence of radiation they define an allowed region in the hadronic (energy,mass) plane which has roughly the shape of a triangle for a vanishing neutrino mass (in fact it is exactly a triangle in the plane ($\frac{E_{had}}{E_{beam}}$ vs $(\frac{m_{had}}{m_\tau})^2$). If the neutrino had a mass the edge of the triangle would reduce to a smooth curve.

Of course an analogue formula holds for the 1-dimensional case, this one being also unaffected by the radiation. In both cases final state radiation has been neglected.

3 The theoretical distribution

The theoretical distribution (up to constants) is made of two parts : the matrix element and the phase space factor. The hadronic tensor of the matrix element is :

$$H^{\mu\nu} = (g^{\mu\nu} - \frac{q^\mu q^\nu}{q^2})h_1(q^2) + q^\mu q^\nu h_0(q^2)$$

where $h_{0,1}(q^2)$ are the structure function for a spin 0(1) hadronic system.

In general, as the W has spin 1, scalar states are suppressed and would be forbidden in the limit of vanishing masses. It is possible to show that the suppression is also a function of the parity of the state and that scalars are suppressed like $\frac{(m_u - m_d)^2}{q^2}$ and pseudoscalars like $\frac{(m_u + m_d)^2}{q^2}$ [5].

For n=5 a spin 0 state with L=0 (the simplest choice) should be a pseudoscalar with odd G parity similarly to the π which is $J^{PG} = 0^{--}$. However there are no known $'\pi - like'$ suitable (i.e. having a mass smaller than the τ mass and decaying in 5 π) resonances that could dominate the scalar production.

The spin 1 state should be a $J^P I^G = 1^+1^-$ resonance (like the a_1); here as well there aren't suitable resonances. Therefore it is most likely that the 5 pions are grouped by two or three in such a way to form a J=1 state.

Following the above arguments the term in $h_0(q^2)$ has been neglected and $h_1(q^2)$ has been taken either as a constant (pure space phase approximation) or as a $\rho(a_1)$ Breit-Wigner function convoluted with the space factor for the decay $\tau \to \rho 3\pi\nu, \rho \to 2\pi$ ($\tau \to a_1 2\pi\nu, a_1 \to 3\pi$).

The curves for these three hypothesis are shown in fig. 1. The difference between them is small and the use of one or the other will be considered in the systematics. The plot already suggests that the better limit will come from the a_1 curve as in this case there is less phase space left free for the neutrino, while the pure phase space approximation will give the uppermost limit.

In the n=6 case the spin 0 term has also been neglected because no scalar with positive G parity can be produced in a τ decay being CVC forbidden.

The spin 1 state should be a $J^P I^G = 1^- 1^+$ (like the ρ). The existence of one or even more of such a state (the ρ') is not settled yet. Candidates with masses ranging from 1300 to 1700 MeV have been proposed by several e^+e^- and fixed target experiments, but no clear picture has ever emerged.

Even without assuming a particle dominance one could think to use CVC to relate the $h_1(q^2)$ to a suitable combination of the e^+e^- cross sections, in analogy to what is done in the case of n=4. Unfortunately the analysis of the isospin independent amplitudes [6] shows that this is not possible because there are four of such amplitudes and only three observable cross sections ($e^+e^- \to 6\pi^0$ is forbidden). Moreover only two of these have been ever measured. Therefore also in this case the pure phase space approximation has been taken.

Once the choice of $h_{0(1)}$ has been made the calculation for $\frac{d\Gamma}{dm}$ and $\frac{d^2\Gamma}{dmdE}$ is straigthforward. In the pure phase space case we have used an analitical approximation [7] which strongly reduces the computation time of the fit; for the other two hypothesis where the convolution with the appropriate Breit-Wigner had to be taken this was not possible. In fig. 2 we show the function in the (E_{had}, m_{had}) plane with and without radiation, together with the Koral06 prediction. The fraction of events falling out the 'no-radiation' kinematical limit is 3.7% according to our calculation and (4.2 ± 0.3)% according to Koral06.

4 Event selection

The event selection is made in four steps :

- TSLT01 is used and the event is divided into two hemispheres using the thrust axis made with the Energy Flow;
- a 5*prong* event selection is applied by the following criteria :

  1) 5 *good* tracks and 0 *bad* tracks in the *5 prong* hemisphere;
  2) $\sum_{i=1}^{5} q_i = \pm 1$ in the *5 prong* hemisphere;
  3) $\sum_{i=1}^{5} |d_0| < 0.8cm$ in the *5 prong* hemisphere;
  4) less than 6 tracks (*good* + *bad*) in the *opposite* hemisphere;
  5) invariant mass of the *opposite* hemisphere (tracks+photons) $< m_\tau$;
  6) total charge of the event (*both* hemispheres) ≤ 1,
  7) less than 3 photons in the *5 prong* hemisphere;

where a *good* track is a track with $|d_0| < 1cm$, $|z_0| < 10cm$, $N_{TPC} \geq 4$ points, $|cos(\theta)| \leq 0.95$ and $p \geq 100MeV$, it is not identified as an electron by Taupidx [8] and does not enter any combination compatible with a photon conversion; and a *bad* track is any remaining track;

- 5π and $5\pi\pi^0$ events are selected out of previous sample requiring :

  a) for the $\tau \rightarrow 5\pi\nu$ sample :
  $N_\gamma(good) = 0$,
  $N_\gamma(bad) \leq 1$;

  b) for the $\tau \rightarrow 5\pi\pi^0\nu$ sample :
  $N_\gamma(good) = 2$,
  $N_\gamma(bad) = 0$,
  $N_{\pi^0} = 1$,
  $R1_{\gamma 1} > 0$,
  $R1_{\gamma 2} > 0$;

  a *good*, a *bad* photon and a π^0 are defined as in Pegasus [9];

- eventually a cut on the invariant mass of the $5\pi(5\pi\pi^0)$ system is applied at $m < 2.5GeV$.

The aim of the selection is not to maximize the efficiency but to avoid as much background as possible in the selection. The $non - \tau$ background originates from $q\bar{q}$ and llV events where $l = \tau$, while the τ background comes from misclassification of the τ decay modes. In this aspect it is important to avoid those contaminations that could mimick a zero mass neutrino. For example a $\tau \rightarrow 5\pi\nu$ decay classified as a $\tau \rightarrow 5\pi\pi^0\nu$ would induce a better limit on the neutrino mass while the opposite error of classification would mimick a massive neutrino. As we are willing to put an upper limit the second kind of background can be tolerated but the first should be suppressed.

The efficiency of the selection and the background from τ events have been investigated using about $200K$ events of the last MC production, 5000 $\tau \rightarrow 5\pi\nu$ and 5000 $\tau \rightarrow 5\pi\pi^0\nu$ events of a dedicated production. The efficiencies of the selection and the contamination of the selected samples from τ background are shown in table 1.

	5π	$5\pi\pi^0$	$K^0_s K^0_s \pi$	nucl. interactions
5π	26.1 ± 0.6	7.1 ± 0.7	2.9 ± 2.0	0.07 ± 0.06
$5\pi\pi^0$	2.6 ± 0.8	8.4 ± 0.4	0	0.23 ± 0.21

Table 1: Selection efficiecies (in %) and contamination of the selected samples(in %) from τ background for each of the two modes

channel	Exp. events $\sigma_{peak} * \int L$	MC sample	After TSLT01	After 5 prong sel.	After $m < 2.5GeV$ cut
$\tau\tau ee$	109	1000	470	0	0
$\tau\tau\mu\mu$	36	1000	339	11	1 (m_h=2.49 GeV)
$\tau\tau\tau\tau$	3	1000	162	2	0
$\tau\tau u\bar{u}$	47	1000	264	6	0
$\tau\tau d\bar{d}$	13	1000	245	5	2 (m_h=2.3,2.2 GeV)
$\tau\tau s\bar{s}$	8	500	130	2	0
$\tau\tau c\bar{c}$	13	1000	45	1	0
$\tau\tau b\bar{b}$	2	1000	0	0	0

Table 2: Background from llV events

For the background from $non-\tau$ events we have used 7500 llV events [10] in the configuration $\tau\tau f\bar{f}(f = e, \mu, \tau, u, d, s, c, b)$, about $1750K$ $q\bar{q}$ events and an *ad-hoc* production of $q\bar{q}$ events in the $5-1$ topology (where all long-living particles were forced to decay) corresponding to about $6M$ hadronic events.

The result on the llV events are resumed in table 2; 27 events corresponding to about 0.8 events in the data sample pass the *5 prong* selection. All them have masses greater than 2.5 Gev except three that have $m_{had} = 2.2, 2.3, 2.49GeV$. The mass distribution is shown in fig. 4 together with the MC for the signal and the data.

Note that the potentially most 'dangerous' background comes from the $\tau\tau\mu\mu$ events. Out of the 11 that survive the 5 prong selection 7 have two identified muons in the *5 tracks* hemisphere, 2 have 1 identified muon (m_h=13.3,5.6 GeV) and 2 no muon at all (m_h=4.2,4.1 GeV).

Out of the 1750 K hadronic events only 7 events survive up to cut 3). All of them fail the cut at 2.5 GeV invariant mass, 6 have more than 2 photons in the *5 prong* hemisphere and 1 fails both cuts 4) and 6). This means that the expected background is at least smaller than one event.

Out of the dedicated hadronic production 4 events survive up to cut 3). Two of them fail the cut at 2.5 GeV invariant mass as well as cuts 5) and 7); one is rejected by the $5\pi(\pi^0)$ selection and one survive all the cuts. The surviving event is a $Z \rightarrow s\bar{s}$ event with $m_{had} = 1.69GeV$, $E_{had}/E_{beam} = 0.62$, which is outside the allowed '*no radiation*' region. This is an indication that there is no physical channel mimicking the signal topology able to contribute more than 0.3 events of background. Therefore it is reasonable to expect that the hadronic background -if any- is uniformly distributed rather than peaked in the high mass/high energy region (for example coming the D^0 decays) as one could have feared.

If the background distribution is assumed flat the contribution expected in the region with $1.67GeV < m_{had} < 1.77GeV$ and $0.95 < \frac{E_{had}}{E_{beam}} < 1$ (the top corner of

After cuts 1,2	After cut 1,2,3	Up to cut 6	Up to cut 7	Up to $5\pi(\pi^0)$ selection	All cuts
62	54	50	38	24(4)	23(3)

Table 3: Effect of the different selection requirements on the data sample.

the allowed '*no radiation*' signal region where the sensitivity to the neutrino mass is much higher) is less than 0.002 events.

When the selection is applied to the 1991+1992+1993 data 26 events survive the selection, 23 are classified as $5\pi\nu$ and 3 as $5\pi\pi^0\nu$. We list in table 3 how the different cuts are effective on the data and in table 6 (at the end of the note) the main characteristics of the 26 remaining events. Two events are discarded because they have a mass bigger than 2.5 GeV; from visual scanning one of them(m_h=17GeV) looks like an llV event (with two muons in the *5 prong* hemisphere) and the other(m_h=2.9GeV) shows a track very far in z_0 from the other four, probably because of a nuclear interaction. No event is found in the region between the τ mass and 2.9 GeV.

For all the 26 events surviving the full selection the total charge is zero. Only one event (event 4) has one track identified as a muon in the *5 prong* hemisphere. All events but event 10 have one track in the *opposite* hemisphere.

5 Correction to track momenta

A recent investigation on tracking [11] using $K^0_s \to \pi^+\pi^-$ has shown that the K^0 mass is not well reconstructed for K^0 momenta below 3 GeV. The observed shift in the data is about 4 MeV at low momenta and rapidly decreases to zero. A similar effect holds also for $\Lambda_s \to p\pi$.

The effect was ascribed to the underestimation of energy losses in the walls of the subdetectors and succeffully corrected with an *ad hoc* function $f(\beta, \theta)$ applied to single particle momentum. We have applied the same correction [12] and found a small but significative increase in the invariant hadronic masses ranging between 0.3 MeV and 1.3 MeV.

6 Determination of E_{had} and m_{had} MC resolution

For each event the error on the invariant mass, the error on the energy and the correlation coefficient have been computed with a long but straightforward propagation of the errors on the 3(6) momentum parameters $\rho, tg\lambda, \phi, (E_{\pi^0}, \theta_{\pi^0}, \phi_{\pi^0})$. The correlations between the parameters of a single track, as given by Julia, have been included

in the propagation, while the parameters of different tracks have been assumed to be uncorrelated.

However this procedure underestimates the error on the invariant mass by an average factor of about 1.4 ± 0.1 as shown in fig. 7. There we plot the invariant mass resolution in unit of the σ computed propagating the Julia errors. The curve is roughly consistent with two gaussians with an additional tail. The central gaussian contains about the 70% of the events, it is centered on zero and has a width of about 1.4. The second gaussian is much broader and slightly shifted to positive values, which means that the mass is overestimated by about $(0.6 \pm 0.2)\sigma$ (the mean value of σ is about 13 MeV).

The presence of a second gaussian should not be a surprise because the invariant mass is not a linear function of the track parameters. We have built a toy MC to compute the relevance of the second gaussian by assuming that the input parameters are gaussianly distributed (which is not completely true) around their true value with a nominal σ. This crude assumption reproduces the bulk of the resolution in a remarkable way, as shown in fig. 8 where we have plotted the mass resolution in GeV (previous to the 5π selection). The complete MC however shows longer and asymmetric tails.

The influence of nuclear interactions on these tails has been investigated with a dedicated MC production where both elastic and anelastic nuclear interactions were switched off in Geant (actually the effect of anelastic interactions is expected to be negligible because such events are rejected by the event selection). No sizeble difference with the full MC simulation was noticed.

It is mostly natural then to ascribe these tails to tracking problems, in particular to hit mis-assignements.

The correlation with the sum of the χ^2 of the Julia fit of the tracks is shown in fig. 9: as expected at low values of χ the offset is smaller and the second gaussian contributes less, but no strong dependence is evident.

To take in account the above effects for the data we created several hundred copies of each data event in a 'Kine' format and processed them through the entire Galeph+Julia+Event Selection chain. In this way it was possible to derive the correction factors to the computed σ and to the offset of both the mass and energy resolutions. The factors were obtained by fitting the curves of the 'cloned' events. The fits were made using a gaussian plus a flat tail. The mass correction factors agree well with the average 1.4 expected; the energy correction factors agree with the expected average of 1. As examples we show the plots of the most significative (for the mass fit) events (events 1,8,15,18) in fig. 11 and 12. Few events (events 1,2,11,15,20) show a small (few MeV) offset in the mass towards higher values. We have considered such offsets in determining the systematics.

7 Vertexing

Vertexing the five charged tracks to a common vertex has been done using the standard YTOP package. All events but one show a vertex whose position in the $x-y$ plane is shown in fig. 13. The χ^2 of the fit is shown in fig. 14. The event which does not have a five tracks vertex (event 10) shows on the contrary a three tracks vertex with d_{xy} compatible with the beam pipe radius. We have then rejected the event considering it as a nuclear interaction with the beam pipe wall. The mass reconstructed after the vertexing of the tracks is shown in fig. 15. Here again the mass resolution is reasonably fitted with a double gaussian. However the second one is extremely displaced, resulting in an underestimation of the mass of about 2.5σ. For this reason we have used the vertexing issue only to check the position of the five tracks vertex but we have not used the invariant mass value in the neutrino mass fit. In fig. 16 we show the Julia error on the mass vs the YTOP error. The plot shows that the gain in the size of the errors using the vertexing would be marginal.

8 Result of the fits

The two fits were performed on the remaining 25 events. To cross check the numerical precision of the various integrals in the likelihood computation we compared three different Cern library integration routines. The most delicate integral is the one involving the radiation because it convolutes a function with a singularity at the integration limit (corresponding to the infrared divergency of soft photon emission). We estimate the precision on this integral to be better than 2%, while we estimate the precison on the other integrals to be better than 0.1%. The likelihood of the two fits is shown in fig. 17. Both fits converges to zero, the monodimensional one giving a limit of 37.6 MeV and the bidimensional a limit of 23.0 MeV.

9 Systematics

We have considered the following sources of systematics :

- Mass resolution : this has been investigated looking at the recostructed D^0 mass in the decay chain $D^{\pm\,*} \rightarrow D^0\pi, D^0 \rightarrow K3\pi$ (all charged) [13]. This decay is the best suited as it has four tracks in the final state and the Q value is almost the same of $\tau \rightarrow 5\pi$; the energy of the selected D^0 is also relatively high (about $0.6E_{beam}$). Data and MC prediction are shown in fig. 18. The mass distribution is fitted with a gaussian plus a flat tail for the background. The data shown a mass of $(1865 \pm 0.5)MeV$ and a width of (10.3 ± 0.8) MeV that has to be compared with MC values of (1864 ± 0.2) MeV and (8.7 ± 0.5) MeV (input value in the MC 1864 MeV, PDG (1864.5 ± 0.5) MeV). Therefore we have applied a $\pm 0.5MeV$ shift on the mass and a $+20\%$ increase on the mass resolution.

- Energy resolution : we have investigated the energy resolution looking to the reconstructed J/Ψ mass in the decay $J/\Psi \rightarrow \mu^+\mu^-$ [14] and to the D^0 mass in the decay $D^0 \rightarrow K\pi$ (both charged) [15]. In both decays the average opening angle between the daughter tracks is rather large (about 300 mrad and 200 mrad respectively) so that the mass resolution is dominated by the energy resolution. We found $m(J/\Psi) = (3094 \pm 2)MeV$ (PDG $3096.9 \pm 0.1MeV$) and $m(D^0) = (1864.2 \pm 0.3)MeV$. The reconstructed masses are shown in fig. 19 and fig. 20.

  Both measurements are consistent with the expected values and therefore they give an upper limit on the energy systematics. Assuming a systematic error on the momentum of each single track of the form $\Delta p = k*p$ the above discrepancies require a factor $k = 0.065\%$ for the J/Ψ and $k = 0.027\%$ for the D^0. The extrapolation at 45 GeV of the D^0 correction would give an error of 12.1 MeV on the energy measurement.

  The above procedure is -at first approximation- insensitive to subdetectors misalignements or distortion in the electric field that give charge dependent systematic effects. These are investigated looking at the muon energy distribution in $\mu^+\mu^-$ events. From the E_μ/E_{beam} curves one can estimate an error of about 12.5 MeV. This means that charge dependent effects in the $\tau \rightarrow 5\pi(\pi^0)\nu$ system are of the order of $2-3$ MeV which is much smaller than the charge insensitive contribution.

- Mass-Energy correlation : this is the most difficult point to investigate. The average opening angle between the pions in $\tau \rightarrow 5(6)\pi\nu$ is about 50 mrad so that the error on the mass receives a contribution also from the determination of the tracks direction. However we have assumed a conservative attitude and applied an arbitrary combined shift of $0.5MeV$ on the mass and $(0.027\%)E$ correction on the energy as if they were 100% correlated.

- Beam energy : a correlated error of 6 MeV coming from absolute energy calibration and an uncorrelated error of 37 MeV coming from run conditions has been applied to the beam energy of each event following the energy calibration group indications [16];

- τ mass : the value of the mass has been taken to be $m_\tau = (1777.0 \pm 0.5)MeV$

- τ lifetime : we have investigated the effect of the lifetime on the tracking parameters with the MC. We found that they are negligible for both the mass and the energy determination.

- Theoretical function : the fits have been done using the pure phase space approximation. The $\rho + 3\pi$ and $a_1 + 2\pi$ distributions have been used to check the influence of the model.

- Background : we expect the background to be negligible.

- Fit stability : we have listed in table 5 the variation of the results once one of the most important events at the time is taken out from the fit.

A cross check on the sensitivity of the fit has been also done with a dedicated production of events in which the neutrino mass was set to $m_\nu = 30 MeV$. With 180 of such events and average correction factors (without reproducing each event several hundred times like we did for the data) we obtain $m_\nu = 29^{+18}_{-29} MeV$ (1σ) for the mondimensional fit and $m_\nu = 34^{+12}_{-34} MeV$ (1σ) for the bidimensional fit. This result shows that the fit is sensitive to a massive neutrino with a good accuracy.

Table 4 summarizes the effects of the above systematics on the fits.

systematic source	variation	1d vararіation (MeV)	2d variation (MeV)
tracking (MC)	offset on events 1,2,11,15,20	+2.2	+0.6
tracking (DT)	± 0.5 MeV mass offset	$^{-0.2}_{+0.2}$	$^{-0.2}_{+0.2}$
tracking (DT)	+20% mass resolution	+2.0	+0.2
tracking (DT)	$0.027\%E$ energy offset	-	+0.2
tracking	mass & energy offsets	-	+0.3
τ mass	±0.5 MeV	$^{+0.5}_{-0.4}$	$^{+0.2}_{-0.1}$
E_{beam} calibration	± 6 MeV	-	+0.1
E_{beam} spread	± 37 MeV	-	+0.3
$\rho + 3\pi$	-	-0.3	-0.2
$a_1 + 3\pi$	-	-0.5	-0.3
total		3.0	0.8

Table 4: List of systematics for the fits

	1d variation(MeV)	2d variation(MeV)
event 1	+8.8	+5.3
event 18	+6.8	+3.2
event 4	+1.2	+1.0
event 15	+0.2	+2.3
event 8	+0.8	+1.6

Table 5: Variation in the mass limit when one event is taken out of the fit.

As all them are uncorrelated we have summed them up in quadrature and added the result to the fit limit to obtain the final results :

$m_\nu < 40.6$ MeV at 95% CL for the monodimensional fit

$m_\nu < 23.8$ MeV at 95% CL for the bidimensional fit

Note that the biggest contribution to the systematic error comes from the fact that few events (basically event 1) show a little mass offset when they are reproduced with the MC. However even if the above errors were reduced (for example by a dedicated refitting of the tracks) the final errors would still be rather small. On the other hand it is evident from table 5 that the result would strongly deteriorate if event 1 or 18 were removed from the fit. However there is no indication that this should be the case and we report the numbers for completeness.

We have also made a rough estimation of the chance of obtaining such limit. In order to do that we have computed with the ALEPH MC the expected number of events outside the boundaries of the kinematical *no-radiation* region defined by a given neutrino mass and compared it with the observed number of events. We have chosen the two values of $m_\nu = 25MeV$ and $m_\nu = 35MeV$ because they limit the region that drives the result of the fit. In the first case one expects 2.3 ± 0.2 events and observes 3 ± 1.6, in the second there are 2.5 ± 0.3 events expected and 7 ± 2.3 observed which corresponds to a probability of about 2.5%. It must be stressed that this is a lower limit to the probability because the dinamical model in the MC peaks at lower values of energy/mass with respect to the data.

10 Conclusions

We have determined a limit on the τ neutrino mass of 23.8 MeV/c^2 at 95% CL which represents the best currently available limit. The use of the bidimensional fit has been decisive in obtaining such result. We have considered systematics of various sources deriving them mostly from the data using decays of $D^0 s$ and J/Ψ kindly provided by several collegues. For all sources we found little contributions to the limit. The background from four lepton events and hadronic Z decays has been studied with the MC and found to be negligible.

11 Acknowledgements

We are in debt to many collegues for very useful discussions, suggestions and technical help. In particular we would like to thank A. Rouge for theoretical insight and technical help on numerical integration, M. Pepe for helping in deriving the analitical bidimensional fitting function, P. Janot for providing the llV MC, D. Pallin and M. Maggi for providing the D^0 spectra, D. Rousseau for the J/Ψ, D. Brown for the low momentum correction and many precious hints, G. Capon for the $q\overline{q}$ background and A. Antonelli, J. C. Briant, J .Raab, L. Rolandi and H. Videau for profiting discussions.

References

[1] ARGUS Collaboration, H. Albrecht et *al*,
Phys. Lett. B 202 (1988) 149, Phys. Lett. B 291 (1992) 221

[2] CLEO II Collaboration, D. Cinabro et *al*,
Phys. Rev. Letters 70 (1993) 3700

[3] J. Raab, L. Bauerdick, Aleph Note 91-121
Upper limit on the τ neutrino mass from $\tau \rightarrow 5\pi^{\pm}(\pi^{o})\nu_{\tau}$ decays
J. Raab, H. G. Sander, L. Bauerdick, Aleph Note 91-139
Upper limit on the τ neutrino mass from $\tau \rightarrow 5\pi^{\pm}(\pi^{o})\nu_{\tau}$ decays (Part II)

[4] Z Physics at LEP 1, Vol. 1, CERN 89-08 (1989)
Z line shape

[5] H. Lipkin, Phys. Lett. B (1989) 226,
Second class currents or simmetry breaking in τ decays

[6] A. Pais, Annals of Physics 9 (1960) 548,
The many π meson problem

[7] E. Byckling, K. Kajantie, Particle Kinematics,
John Wiley & Sons

[8] M. Davier and Z. Zhang, Aleph Note 91-093
Particle identification for tau physics
H. J. Park *et al.*
note in preparation

[9] R. Alemany *et al.*
note in preparation

[10] Courtesy of P. Janot.

[11] D. Brown, Aleph Note 94-046
Tracking studies using K_s^o and Λ_s

[12] Courtesy of D. Brown

[13] Courtesy of D. Pallin.

[14] Courtesy of D. Rousseau.

[15] Courtesy of M. Maggi.

[16] Courtesy of R. Jacobsen

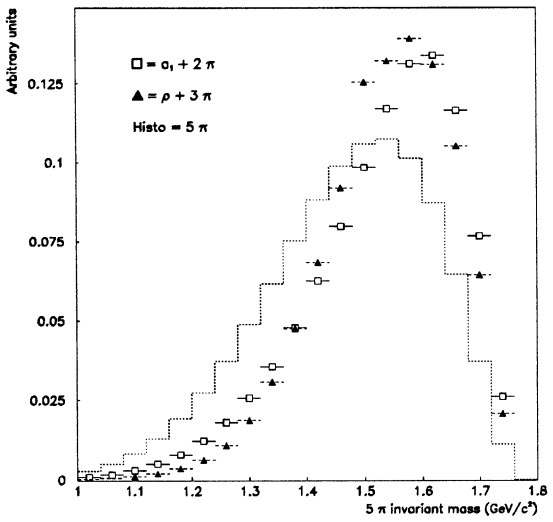

Figure 1: Invariant mass distribution of the 5 pions under the different assumptions: the histogram is the pure phase space approximation used in the fit.

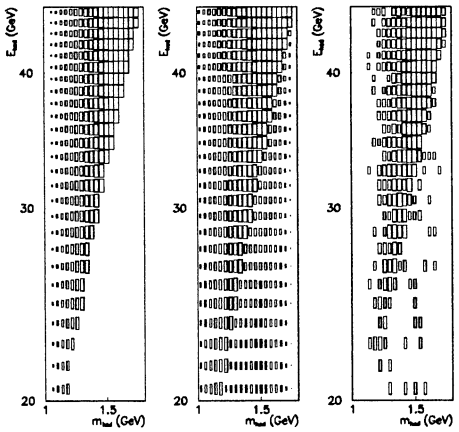

Figure 2: Hadronic energy vs invariant mass : the analitical fitting function (left) without initial state radiation; after convolution with the radiation function (center); the Koral06 MC for about 2000 events(right).

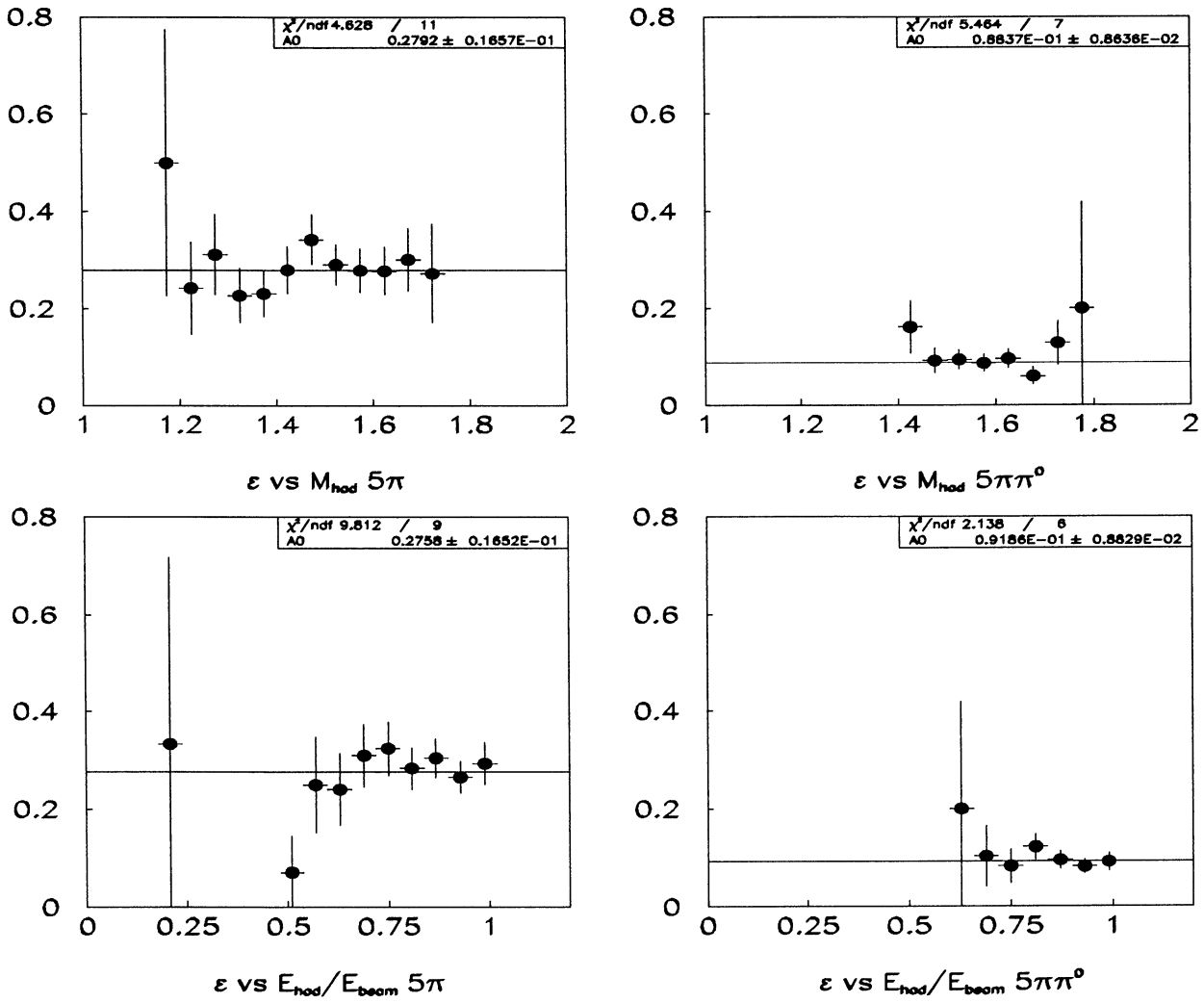

Figure 3: Selection efficiencies vs mass and energy for the two decay modes.

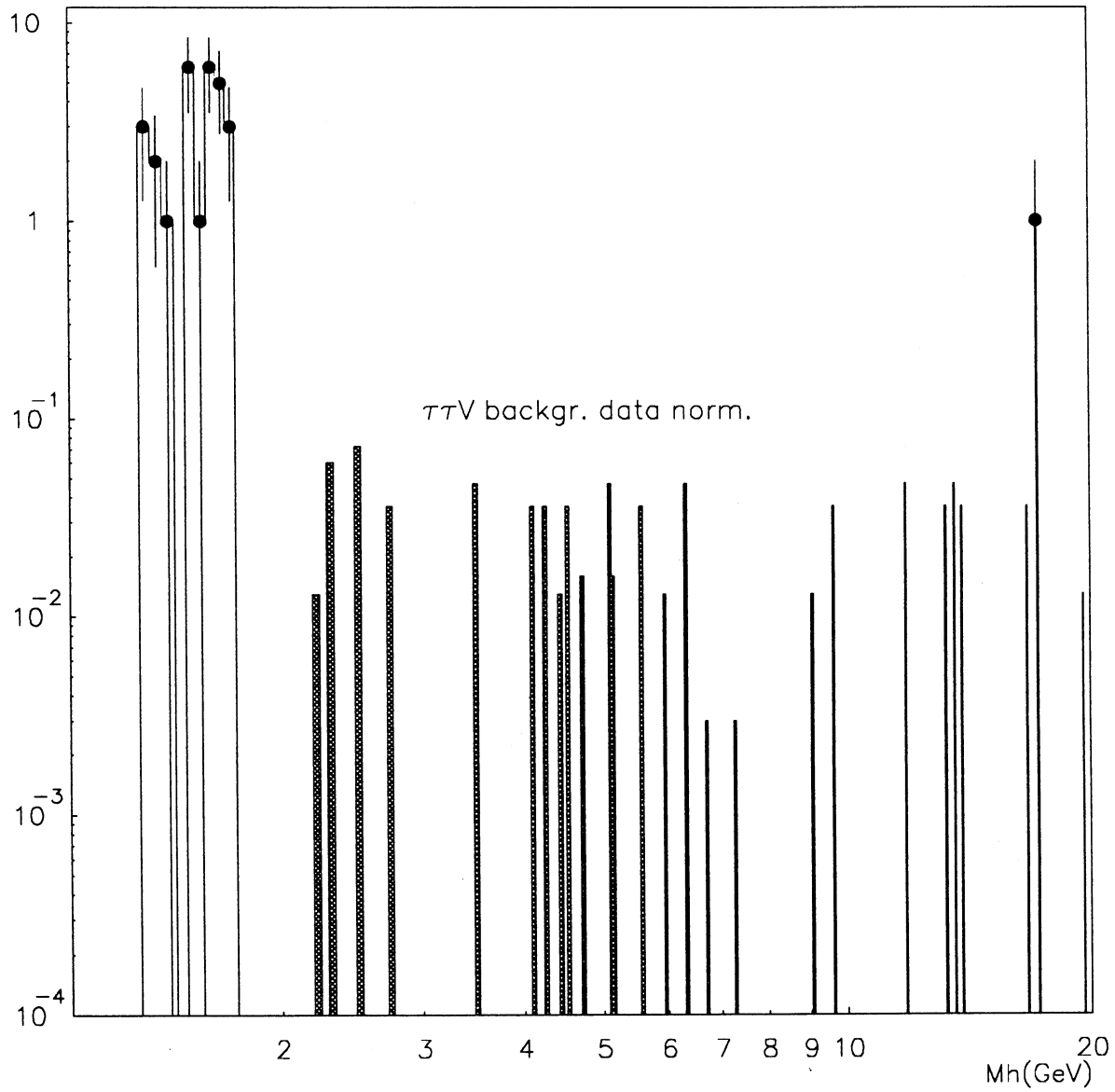

Figure 4: Data(dots) and MC(histo) for the signal and the $\tau\tau V$ background after the *5 prong* selection and previous to the mass cut at 2.5 GeV.

	Run	Event	Mass(GeV)	$Energy/E_{beam}$	ρ	*opposite* side
1	11568	1398	1.738	0.995	0.638	μ
2	11964	4363	1.381	0.758	0.286	$h\pi^0$
3	12297	7016	1.570	0.895	0.297	μ
4	12439	3	1.709	1.046	0.883	e
5	13378	1785	1.664	0.920	0.732	$h2\pi^0$
6	15503	6902	1.394	0.764	0.381	h
7	15937	5336	1.417	0.684	0.364	$h3\pi^0$
8	16395	2682	1.698	0.994	0.716	μ
9	16852	528	1.673	0.894	0.440	h
10	16854	2229	1.725	0.605	0.883	$h\pi^0 K_s^0$
11	16871	8703	1.689	0.959	0.435	$h\pi^0$
12	17248	1101	1.656	0.884	0.525	μ
13	17827	4555	1.554	0.858	0.562	$h2\pi^0$
14	20683	7392	1.534	0.864	0.753	μ
15	20870	9923	1.660	1.000	0.644	$h\pi^0$
16	23139	7572	1.556	0.768	0.546	μ
17	21420	6005	1.346	0.611	0.301	e
18	21428	958	1.744	0.994	0.480	low p
19	21454	3546	1.460	0.703	0.580	$h\pi^0$
20	21483	12323	1.365	0.933	0.273	low p
21	21580	2235	1.593	0.845	0.440	$h\pi^0$
22	21917	2189	1.557	0.879	0.728	μ
23	21978	6838	1.652	0.867	0.739	$h\pi^0$
24	22486	9393	1.536	0.771	0.395	$h\pi^0$
25	22509	7230	1.664	0.899	0.539	$h\pi^0$
26	23077	2499	1.635	0.927	0.504	e

Table 6: Main characteristics of the events surviving the selection. Events 4,10 and 26 are those classified as $5\pi\pi^0$.

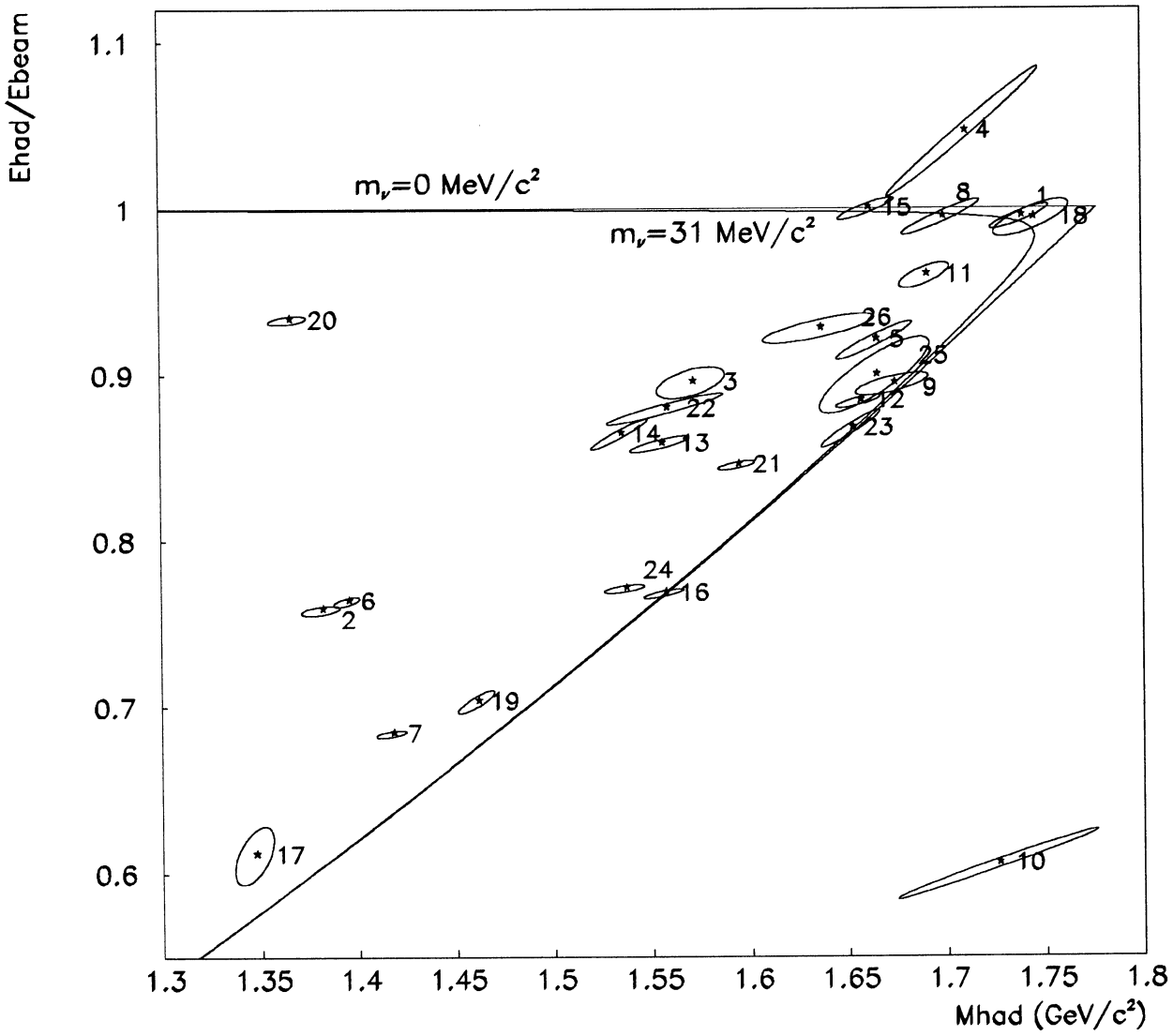

Figure 5: Data events with 1σ contour error. The two lines bound the kinematically allowed region in absence of radiation for neutrino masses of $m_\nu = 0$ and $m_\nu = 31 MeV$; event 10 is not used in the fit.

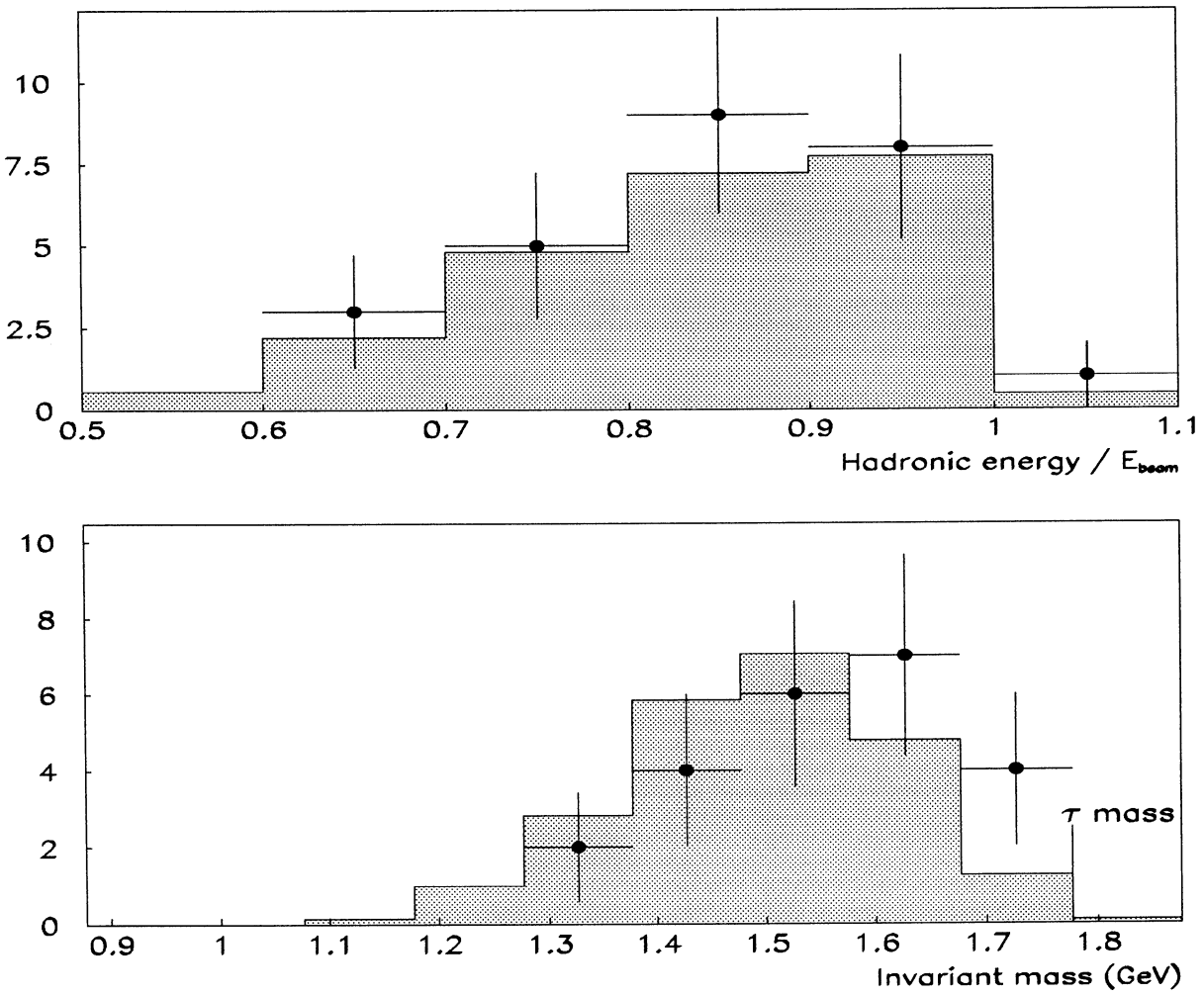

Figure 6: Projection on the two axis for the previous plot (dots) compared with MC predictions (histo) for the 23 $\tau \rightarrow 5\pi\nu$ events only.

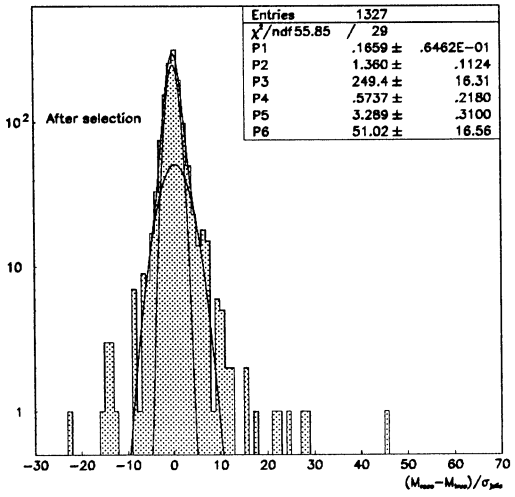

Figure 7: Invariant mass resolution in units of the σ computed propagating Julia errors.

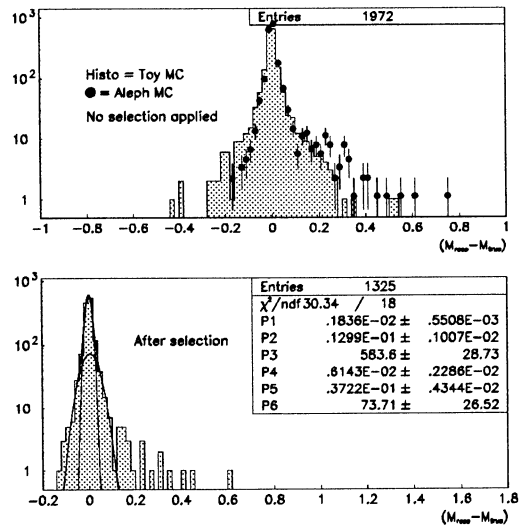

Figure 8: Invariant mass resolution with the toy MC (picture above) compared with the full Aleph MC previous to event selection, and Aleph MC alone after event selection (picture below).

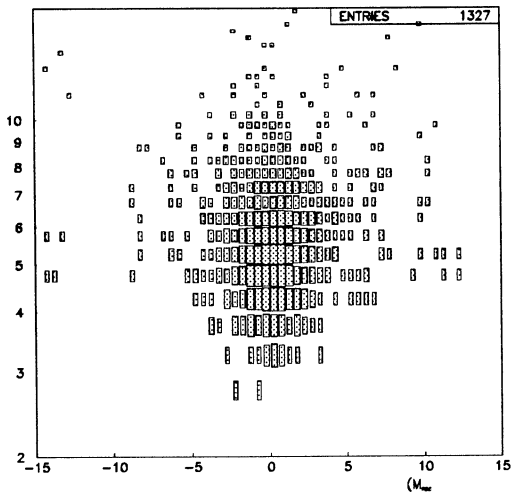

Figure 9: Sum of the χ^2 of Julia tracks vs mass resolution in units of the computed error.

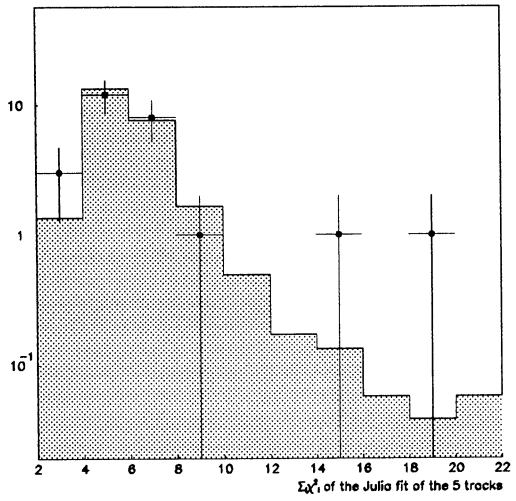

Figure 10: Sum of the χ^2 of Julia tracks for data(dots) and MC(histo).

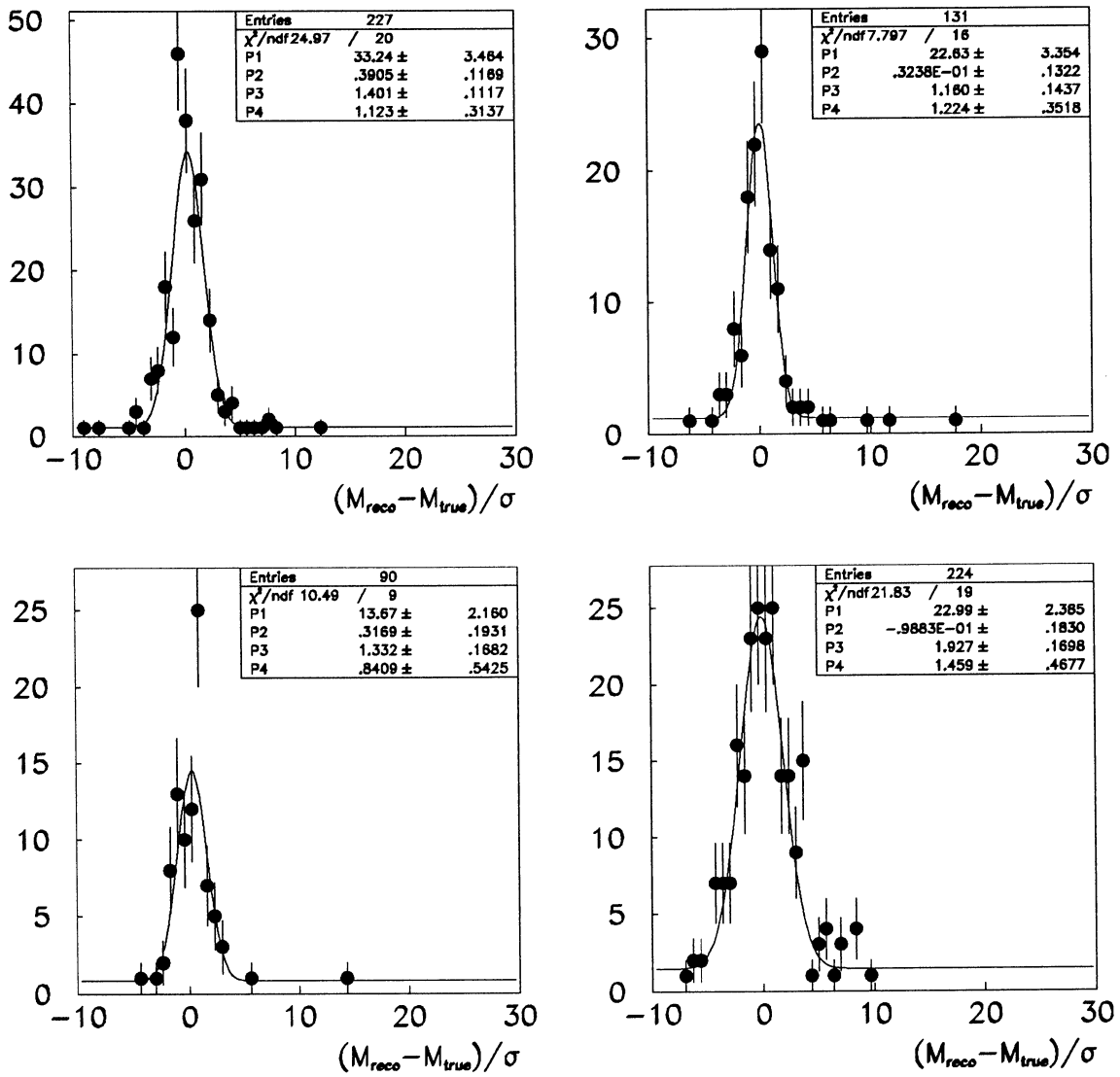

Figure 11: Mass resolution in units of the computed error for the "cloned" copies of events 1 (top left), 8 (top right), 15 (bottom left), 18 (bottom right).

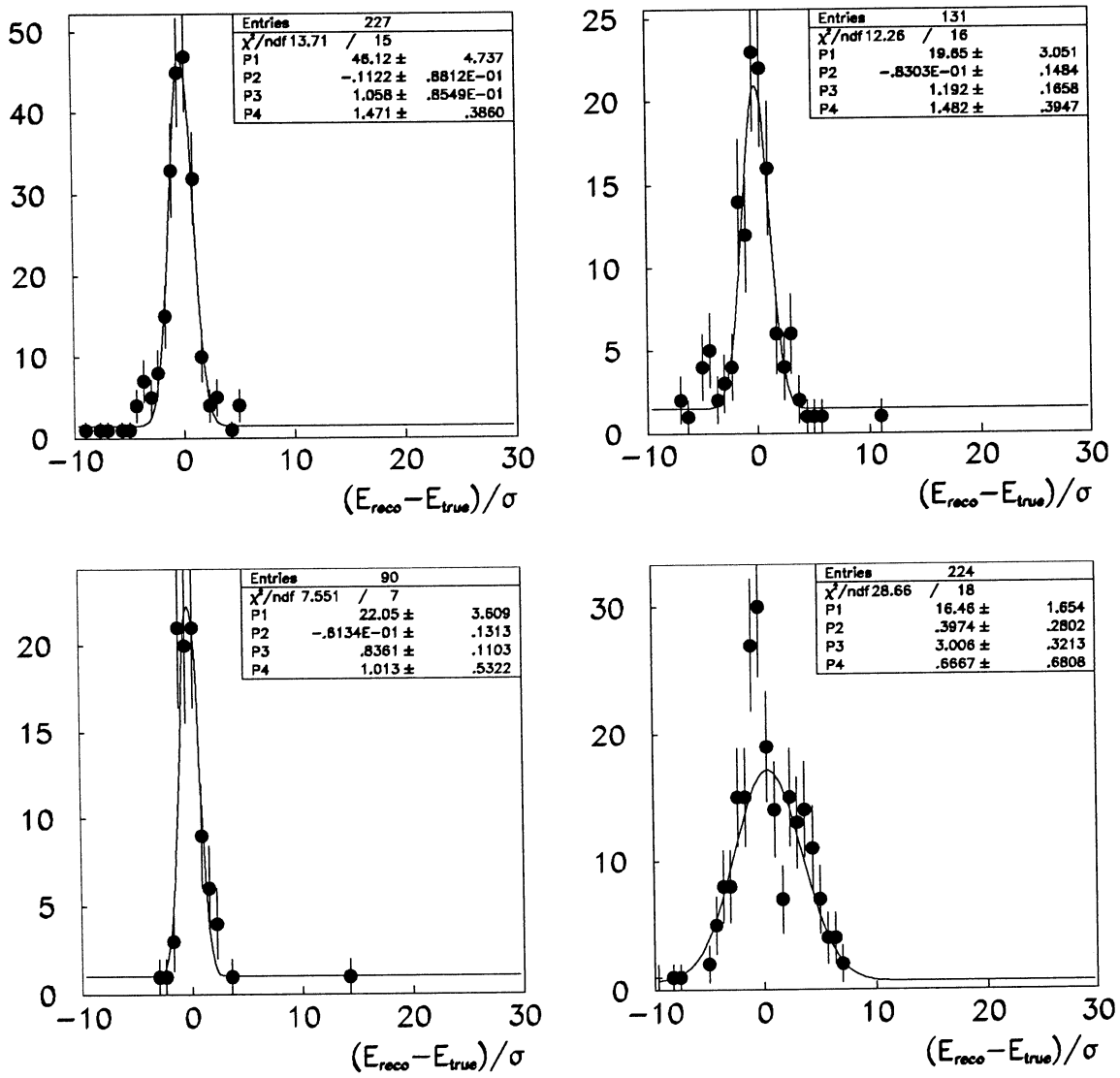

Figure 12: Energy resolution in units of the computed error for the "cloned" copies of events 1 (top left), 8 (top right), 15 (bottom left), 18 (bottom right).

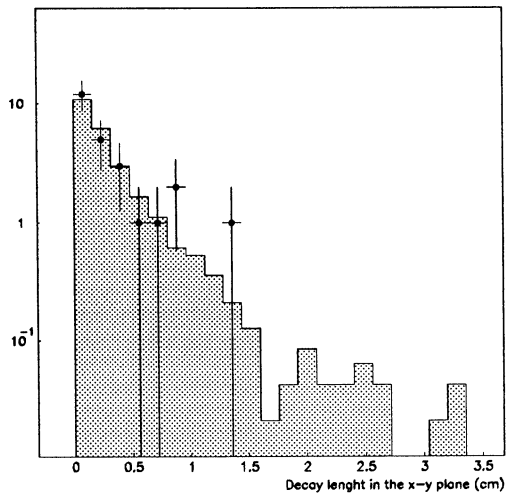

Figure 13: Decay length in the x-y plane for data(dots) and MC(histo).

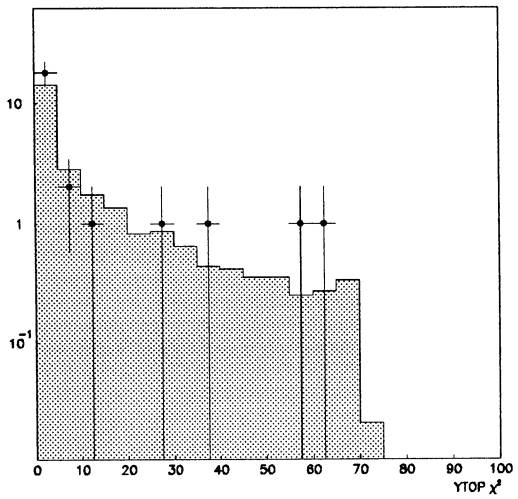

Figure 14: $\chi^2/n.d.f$ of YTOP vertexing in data(dots) and MC(histo).

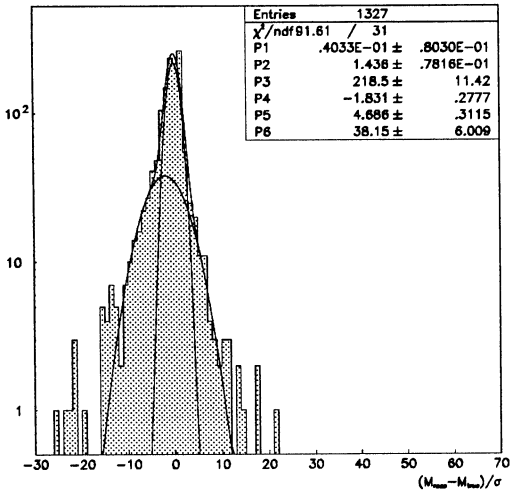

Figure 15: Invariant YTOP mass resolution in units of YTOP σ.

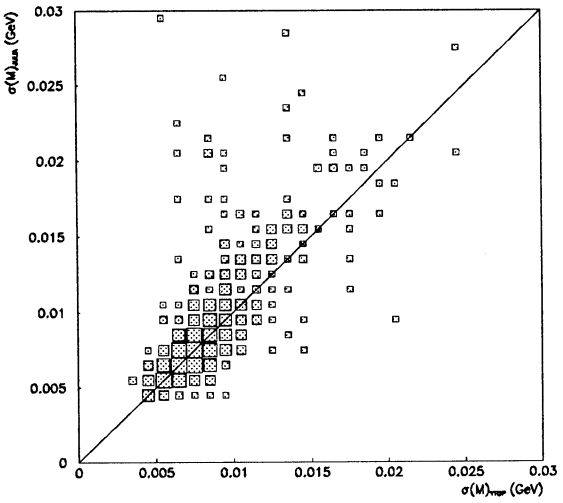

Figure 16: Julia invariant mass errors vs YTOP invariant mass errors.

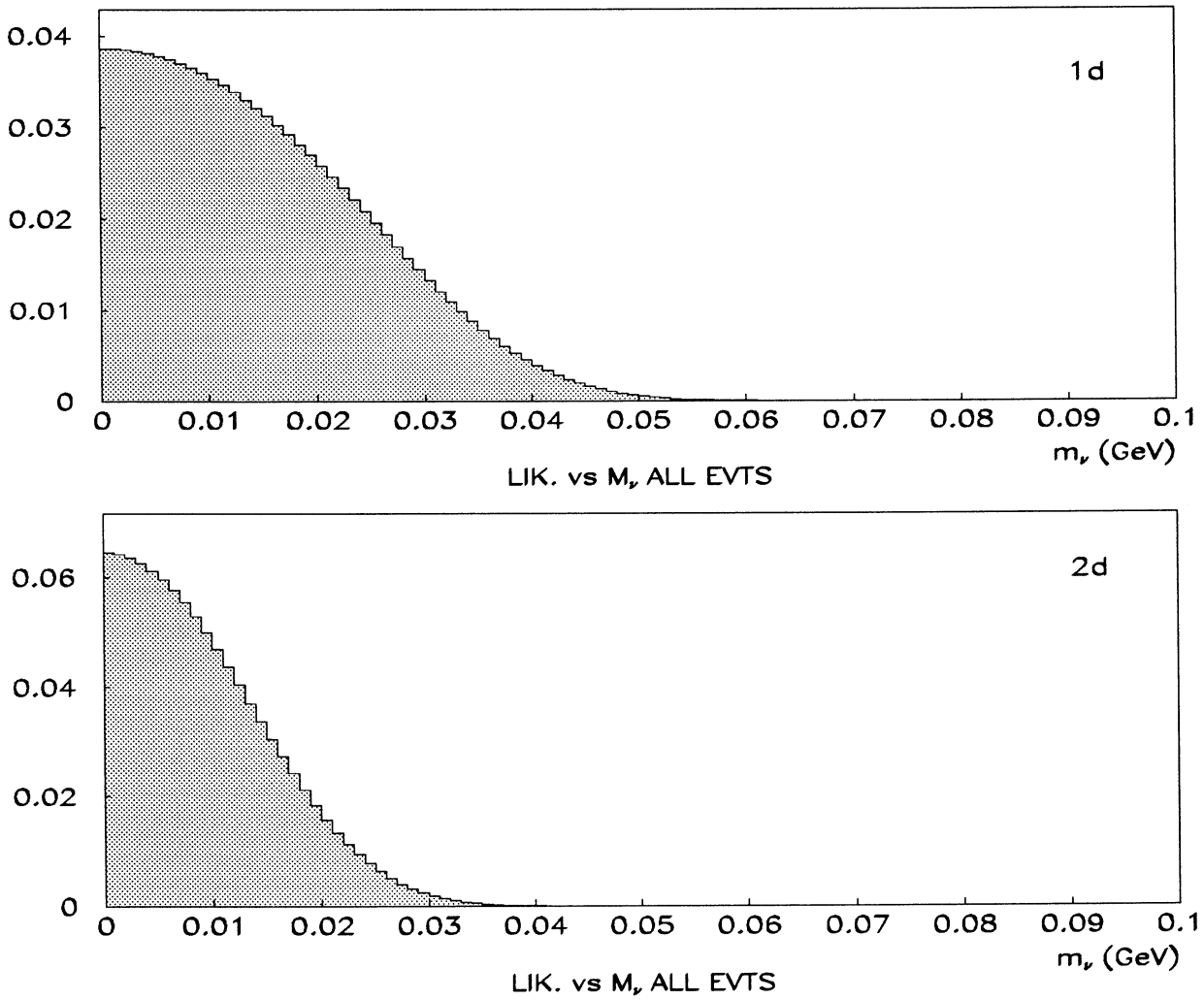

Figure 17: Likelihood of the fits vs m_ν for the monodimensional case (above) and bidimensional case (below).

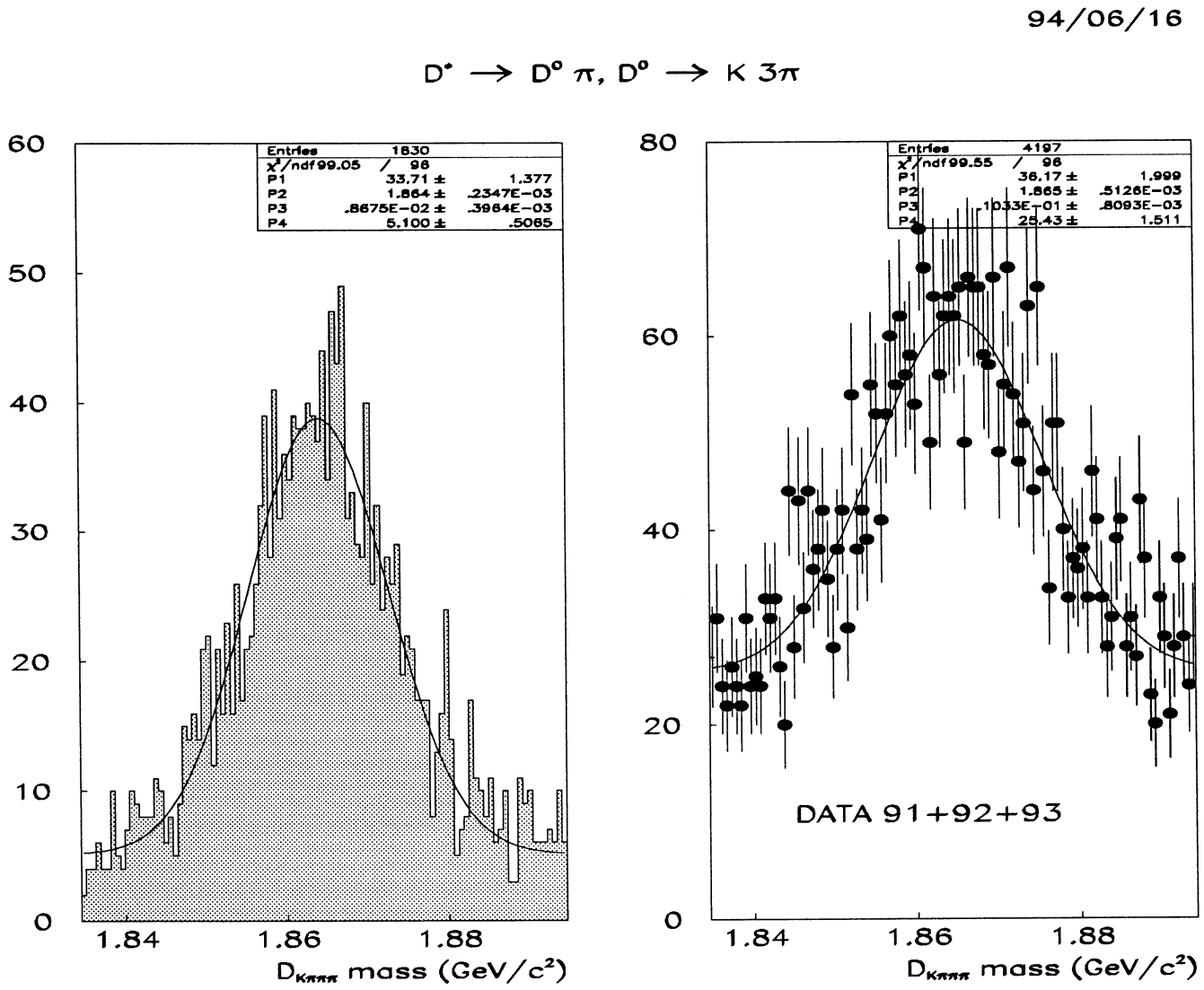

Figure 18: D^0 mass resolution for MC ($c\bar{c}$ only) and data (courtesy of D. Pallin).

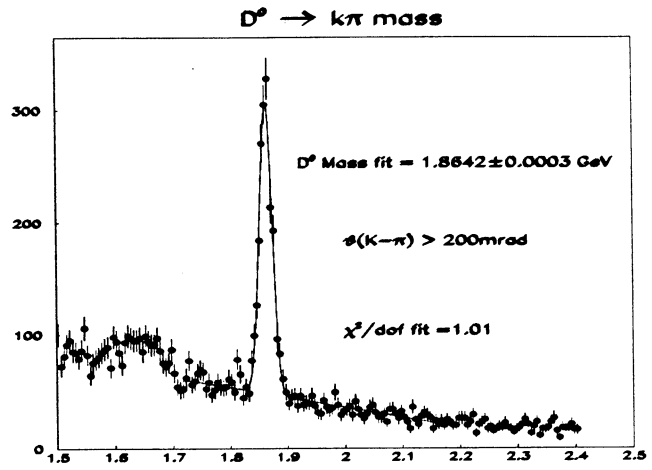

Figure 19: D^0 mass reconstructed in the $D^0 \rightarrow K\pi$ decay (courtesy of M. Maggi).

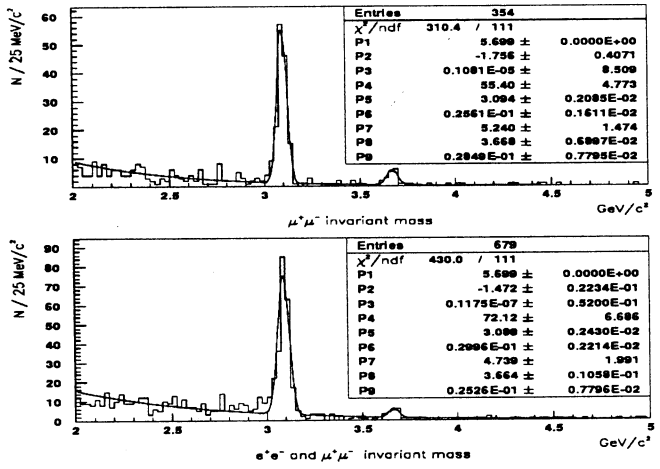

Figure 20: J/Ψ mass reconstructed in the $\mu^+\mu^-$ decay alone as used for the systematics (above) and for both the two leptonic decay modes(below) (courtesy of D. Rousseau).